TPM Vol. 32, No. S8, 2025
ISSN: 1972-6325
https://www.tpmap.org/

Open Access

MULTITUDE EFFECT OF ALUMINIUM SULFATE-DOPED TIO_2 PASSIVATION PHOTOELECTRODE FOR PERFORMANCE ENHANCEMENT OF DYE-SENSITIZED SOLAR CELLS, DSSCS

A.M. SHAHRUL[1], M.H. ABDULLAH[1,2*], M.H. MAMAT[2], N.D. MD SIN[3], E. NOORSAL[1], AGUS SUPRIYANTO[4]

[1]SCHOOL OF ELECTRICAL ENGINEERING, COLLEGE OF ENGINEERING, UNIVERSITI TEKNOLOGI MARA, CAWANGAN PULAU PINANG, 13500 PERMATANG PAUH, PULAU PINANG, MALAYSIA.
[2]NANO-ELECTRONIC CENTRE (NET), COLLEGE OF ELECTRICAL ENGINEERING, UNIVERSITI TEKNOLOGI MARA, 40450 SHAH ALAM, SELANGOR, MALAYSIA
[3]FAKULTI KEJURUTERAAN ELEKTRIK, UNIVERSITI TEKNOLOGI MARA CAWANGAN JOHOR KAMPUS PASIR GUDANG 81750 MASAI JOHOR.
[4]DEPARTMENT OF PHYSICS, POSTGRADUATE, FACULTY OF MATHEMATICS AND NATURAL SCIENCES, UNIVERSITAS SEBELAS MARET, JL. IR. SUTAMI 36A KENTINGAN, SURAKARTA 57126, INDONESIA

Abstract
In this study, aluminum sulphate hydrate, $Al_2(SO_4)_3$-doped TiO_2 based passivation photoelectrode (ADTP) was successfully proved to be a promising method of improving DSSCs. Here, ADTP based photoelectrodes were obtained by varying the percentages of $Al_2(SO_4)_3$ added to the nanoparticles of Titanium dioxide (TiO_2). The morphological images of the ADTPs obtained using field emission scanning electron micrograph (FESEM) indicate their compositional behavior, which include two different sizes (different atomic radii) of titanium and aluminium nanoparticles. Furthermore, the occurrence of the Ti^{4+}/Al^{3+} ions substitution in the ADTP film was then supported by UV-Vis spectroscopy analysis. Meanwhile, the fourier transform infrared (FTIR) spectroscopy analysis revealed that the ADTP samples have higher OH^- functional group which is attributed to the formation of the $Al(OH)_3$ mediators. These mediators enhance the binding of dye molecules to the TiO_2 nanoparticles, thereby improving the adsorption of the dye molecules onto the ADTP surfaces. The subsequent electrochemical impedance spectroscopy (EIS) analysis revealed that all ADTP photoelectrodes exhibited higher conductivity TiO_2 film and trap states, which serves for lower interfacial resistance, inhibiting back recombination and promoting more carriers for electron conduction (photocurrent density, J_{SC}). The integrated properties of the ADTP photoelectrode that improve interfacial resistance, induce higher dye adsorption and reduce back electron recombination resulted in a 0.47 % increase in power conversion efficiency (PCE) of the 3-ADTP-based DSSC.
Keywords: Dye-sensitized solar cell, Aluminium-doped TiO_2 Photoelectrode, mediator, interfacial resistance, back recombination, hydroxyls (OH^-).

INTRODUCTION

Dye-sensitized solar cell, DSSC is a type of photovoltaic technology that converts sunlight into electricity. When compared to other cells, DSSC is less expensive, environmentally benign, and simple to manufacture [1]. TiO_2 is a widely utilized semiconductor oxide either in DSSC photoelectrode or in other domains due to its affordability, lack of toxicity, natural availability, and wide bandgap (2.8-3.3 eV) value [2]. Any modifications that are made to the TiO_2 photoelectrode will affect the properties as well as the performances of DSSC device. As a result, the interface between dye and the TiO_2 has been an interesting topic in recent discussions regarding the fabrication and enhancement of the DSSC [3,4]. As a gauge of merit, the modification of TiO_2 could minimize the quantity of oxygen vacancies on the TiO2 photoelectrode [5] and limit the recombination of charge carriers [6]. The enhancement in dye immobilization uptake on the photoelectrode was accompanied by improvements in conductivity and interfacial resistance, leading to a decrease in the recombination of electrons to their original environment.
Inhibiting the transfer of electrons from TiO_2 to the electrolyte will result in an improvement in terms of photoelectric conversion efficiency (PCE). Three major approaches were used to group the prior research on this topic. In the first method, the blocking layers were made out of very thin layers of inorganic oxides such as MgO [7], ZrO_2 [8], Al_2O_3 [9,10], SiO_2 [11], and Nb_2O_5 [12]. It is the goal of these blocking layers to achieve greater physical passivation between

TPM Vol. 32, No. S8, 2025
ISSN: 1972-6325
https://www.tpmap.org/

Open Access

photogenerated electrons and redox couples, thereby impeding the back recombination process [13]. The second method was to use an acid treatment, which produced a protonation effect on the TiO_2 nanoparticles. This effect made it easier for the dye to be adsorbed, and it reduced the number of electrons that were transferred back to the electrolytes in DSSC [14]. For instance, photoelectrodes treated with nitric acid (HNO_3) have the same effect in terms of producing photogenerated carriers, which contributes to an increase in cell efficiency [15][16]. In the third method, a titanium tetrachloride ($TiCl_4$) solution treatment was used to fabricate a thin layer of TiO_2 on top of a TiO_2 photoanode. This method is a more general procedure when compared to the methods used in the previous two methods. The application of the $TiCl_4$ treatment was based on the idea that a positive shift in the TiO_2 conduction band would lead to a reduction in the electron/electrolyte recombination rate constant [17].

Although numerous passivation techniques such as blocking layer materials, metal oxide doped TiO_2 and acid treatments have been used to combat back recombination. Best to our review, no investigations on the implementation of salt-based passivation material derived from aluminum sulphate hydrate, ($Al_2(SO_4)_3$. H_2O) have been utilized for such purposes yet. $Al_2(SO_4)_3$ salt used in water treatment [18][19] for the purpose of water purification and for dye adsorption enhancer. In most doping procedures and applications, aluminum (metal and oxide form) has been widely utilized as a dopant for TiO_2 [10]. As a result, the purpose of this study is to investigate the application of $Al_2(SO_4)_3$ as a doping material to the TiO_2 nanoparticles for the realization of ADTP photoelectrodes of DSSC application.

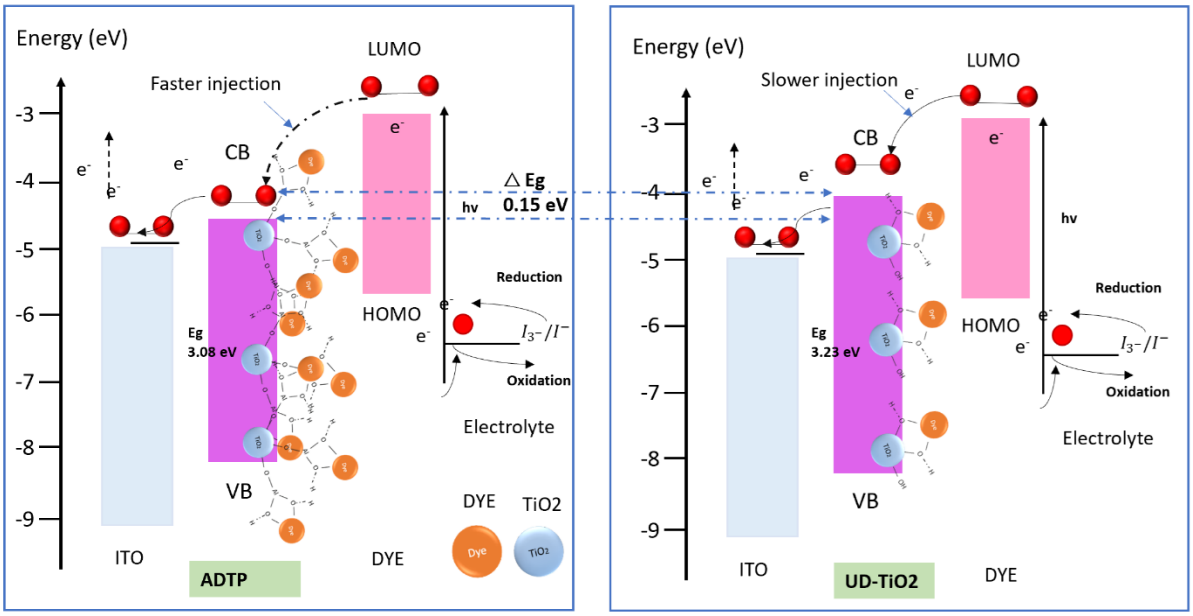

Fig. 1. Band edge position of ADTP cell in comparison to pure-TiO_2 cell

In our prior study, we documented the incorporation of $Al_2(SO_4)_3$ salt as a dye sensitizer additive into the dye sensitizer solution during the dye immersion process. The study revealed that the dye's color intensified and the pH increased in acidity as a result of the direct protonation process of the dye sensitizer. In conclusion, the modified dye has significantly enhanced the overall efficiency of DSSC [29]. However, in this present study we use the same $Al_2(SO_4)_3$ material as the doping material to the TiO_2 nanoparticles during the preparation of ADTP photoelectrodes. As depicted in Fig. 1, we hypothesize that ADTP will be influenced by a conservative acidic reaction occurring on its surface (the dissolution of $Al_2(SO_4)_3$ generates an acidic solution), similar to the effects of an acid treatment procedure. Furthermore, the process of doping regulates the positioning of the band energy and decreases the resistance at the interfaces. These effects result in accelerated electron injection and prevent the occurrence of back recombination in the ADTP photoelectrodes. Last but not least, the influence of the ideal dose of $Al_2(SO_4)_3$ that results in an appropriate quantity of aluminum hydroxide ($Al(OH_3)$). The ideal dose facilitates the coupling of additional dye molecules to the TiO_2 anchor by forming bridges or mediators. For the investigation, Field Emission SEM (FESEM), Raman spectroscopy (Raman), UV-visible spectroscopy (UV-Vis), Fourier transform infrared spectroscopy (FTIR), characteristics of current-voltage (I-V), and electrochemical impedance spectroscopy (EIS) were used to characterize all of these features and characteristics in UD-TiO_2 and ADTP DSSC devices.

2.0 Experiment

2.1 Preparation of TiO_2 Paste (ADTP and UD-TiO_2)

In this method, 10 g of Degussa P25 TiO_2 nanopowder, 20 ml of deionized water, 5 ml of acetic acid, and 5 ml of diluted detergent were blended in a beaker. The detergent was previously diluted by mixing 1 micro spatula of detergent with 20 ml of deionized water. After placing a magnetic stirrer in the TiO_2 mixture and immediately covering

TPM Vol. 32, No. S8, 2025
ISSN: 1972-6325
https://www.tpmap.org/

it with aluminum foil, the mixture was further sonicated for 5 min. The prepared TiO_2 paste was then divided up into five equal quantities and placed in separate small containers. The first container is set aside for the as-prepared TiO_2 paste, which is referred to as undoped-TiO_2 (UD-TiO_2). The remaining four containers were each doped with 0.1g, 0.2g, 0.3g, and 0.4g of alum, and they are referred to as $Al_2(SO_4)_3$-doped TiO_2 (ADTP) in the order of 1-ADTP, 2-ADTP, 3-ADTP and 4-ADTP, respectively. The rest of the experimental section including the DSSCs fabrication and assembly were thoroughly explained in [30].

3.0 RESULT AND DISCUSSION

3.1 FESEM Surface morphology, EDX

The nanostructures of the porous films were obtained from the FESEM image are as shown in Fig.2(a) and (b). Both 3-ADTP, Fig. 2(a) and UD-TiO_2, Fig. 2(b) photoelectrodes have uniform porous morphologies, with only slight variations in their size of surface nanoparticles. The changes in the FESEM surface nanoparticles' size can be attributed to the Al^{3+} substitutional doping (substitution of Ti^{4+} ions by Al^{3+} ions) because of the different ionic radii of both materials [26]. The mixed-size morphology of the ADTP film, which was observed by the FESEM, lends some credence to the idea that the Al^{3+} ions must have been successfully doped into the TiO_2 lattice, creating a mixed structure.

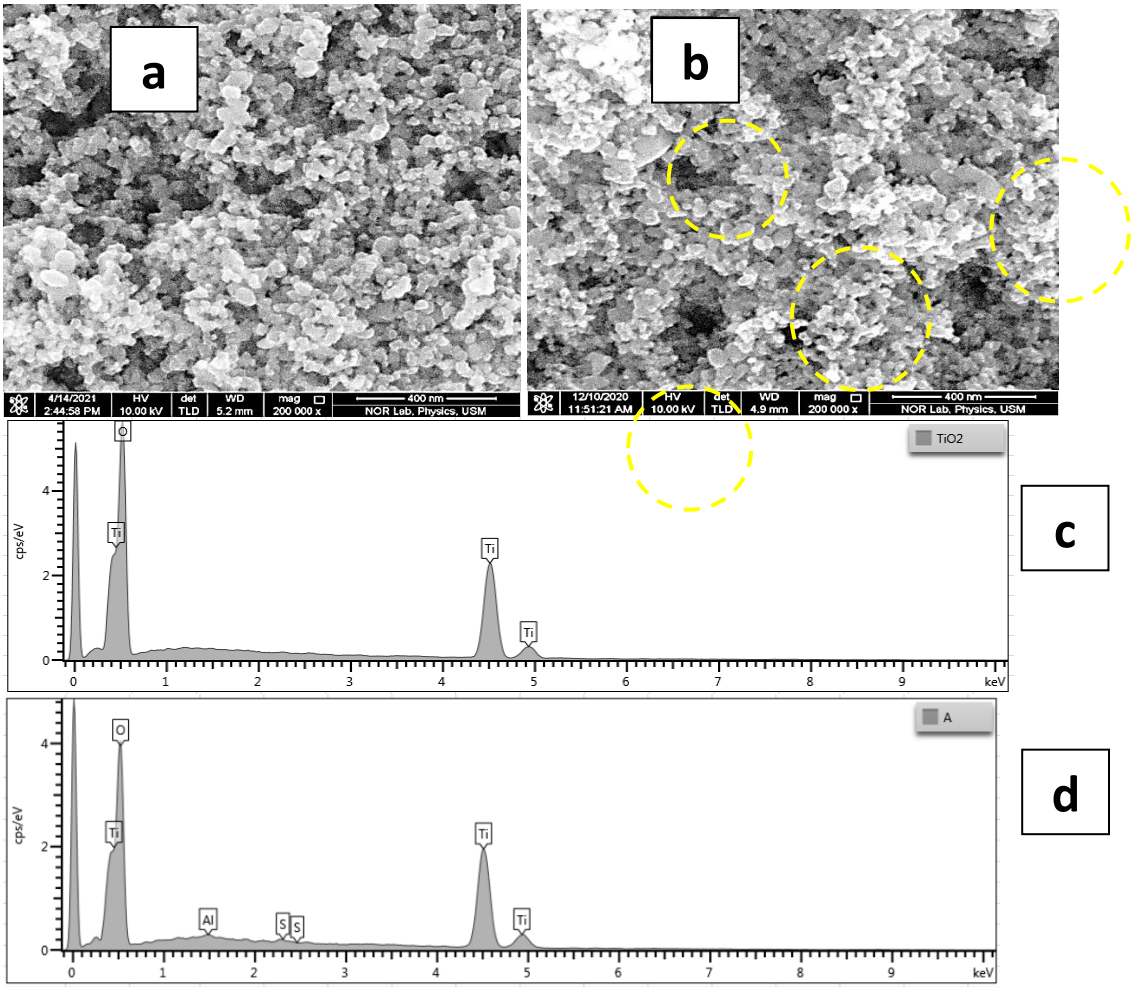

Fig. 2. (a) FESEM morphology of, (a) UD-TiO_2 photoelectrode, (b) 3-ADTP photoelectrode, (c) EDX spectra of UD-TiO_2, (d) EDX spectra of ADTP

3.2 Optical Absorption

For comparison purposes, two absorption spectra between UD-TiO_2 and 3-ADTP films are shown in Fig. 3. According to the spectra, neither of the films has an absorbance that is higher than 400 nm in which the ultraviolet region, UV part displayed most of its high absorbance [20]. The sharp absorbance peaks were observed at a particular wavelength when carriers were shifted from the valence band to the conduction band (V-B to C-B) [21]. In comparison to UD-TiO_2, the UV absorption peak of ADTP film is slightly shifted toward shorter wavelength as a result of the doping of Al^{3+}. Absorbance maxima are shifted towards shorter wavelengths due to a reduction in the bandgap value of TiO_2,

TPM Vol. 32, No. S8, 2025
ISSN: 1972-6325
https://www.tpmap.org/

Open Access

which causes these shifts [22][23]. In this regard, the band gap shift was observed when Ti was replaced by Al^{3+}, which contributes to the modification in the conduction band of the ADTP. The substitution causes defects to be created in the conduction band consequently moves the absorption spectrum closer to the visible region [24].

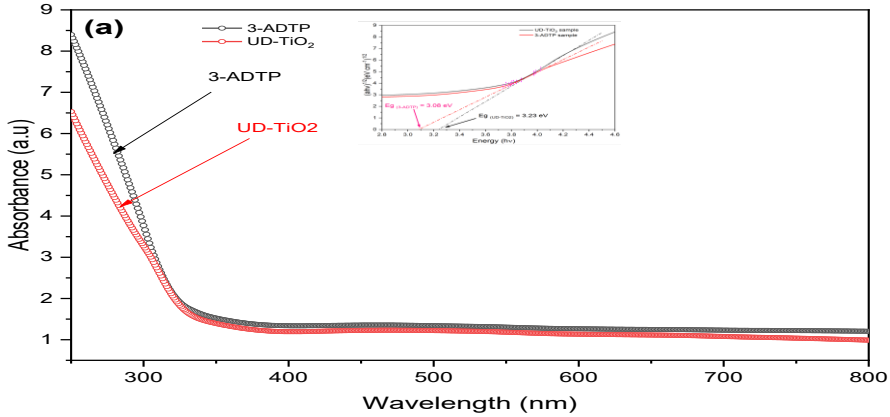

Fig. 3. UV absorption spectra of UD-TiO_2 and ADTP thin film (Inset-Taut plot of both films).

Meanwhile, the inset of Fig. 3 is a depiction of the band gap energy curve for both UD-TiO2 and 3-ADTP, which was determined by using Tauc's relationship. It was seen that the band gap value, Eg of 3.23 eV of UD-TiO_2 is reduced to 3.08 eV when the film is doped with Al^{3+} ions in ADTP. The introduction of impurity energy levels (trap states) within the bandgap by Al^{3+} ions reduce TiO_2's bandgap energy [25]. As the Eg of the doped material (3-ADTP) reduces, thus the transition of the electrons becomes possible within the conduction and valance band of TiO_2 [26]. The blue-shift of TiO_2's absorption spectra as a result of these intermediate energy levels, which was previously discussed in the UV-Vis section, strongly correlates with this [27]. The substitution of Ti^{+4} by Al^{3+} ion causes a decrease in the lattice parameters following Al doping, as conferred in prior Raman measurements. The intermediate energy levels (trap states) generated within the material's bandgap will facilitate electron excitation and transportation. Furthermore, the trapped excited electrons at the interstitial sites help to limit electron-hole pair recombination and reduce interfacial resistance. This may be understood on the premise of concentration quenching effect [28].

In fact, with the increase in doping concentration, more energy levels were created within the band gap and hence band gap energy has decreased [28]. As a result, the ADTP film facilitates the passage of injected electrons from the dye molecules to the TiO_2 conduction band and reduces interfacial resistance of the photoelectrode, resulting in higher performance for ADTP device rather than UD-TiO_2-based device.

3.5 FTIR Spectroscopy

The FTIR spectrum for the UD-TiO_2 and all ADTP samples, after they were immersed in an anthocyanin dye sensitizer is shown in Fig. 4. All samples displayed their essential functional groups in the spectra measured in the range of 400–4000 cm^{-1}. These essential functional groups were vital for dye attachment to the surface of TiO_2 because of their carbonyl (C=O) and hydroxyl (O-H) elements. The O-H stretching that occurs in the hydroxyl group of the anthocyanin dye can be observed between the wavelengths of 2500 and 3500 cm^{-1}, with a peak occurring at 3288 cm^{-1} in the middle of that spectrum [31].

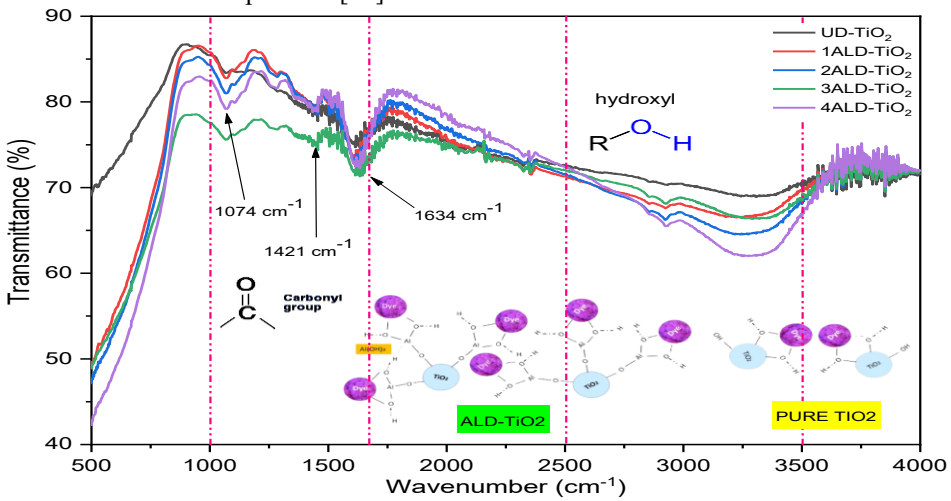

Fig. 4. FTIR spectrum of UD-TiO_2/Dye and four other ADTP/Dye after the immersion process.

Moreover, the appearance of substantially strong sulfate-related peaks in all ADTP samples can be noted at around 1074 cm^{-1}, which agreed with some reported studies of the sulfate bonding occurring between 1000 cm^{-1} and 1200

cm^{-1} [26]. However, these peaks do not represent sulfate ions on their own; rather, it is the appearance of sulfate-related bonding that enhanced the C-O peak of the treated solutions. More interestingly, with the co-existence of surface coverages of hydroxyl groups (O-H) which are known to be reactive can potentially serve as important reactive sites for sulfate adsorption on TiO_2 nanoparticle powdered samples. [46].

Furthermore, the associated hydroxyl functional group of the 4-ADTP sample is found to be the most intense compared to others, which indicates the abundance of dye molecules attached to the TiO_2 nanoparticle. In addition, two additional peaks appeared at 1634 and 1421 cm^{-1} which correspond to the vibrations of the carboxylate molecule's symmetric vsym (-COO-) and asymmetric vasym (-COO-), respectively. These vibration peaks implied for the firmly anchored porphyrin dye to the TiO_2 nanoparticles through bidentate's bridging mode, which includes carboxylic acid from both groups [32]. It is also worth noting that the peak of Ti-OH at 1074 cm^{-1} in all ADTP samples was intensified as $Al_2(SO_4)_3$ concentration increased, indicating that more Al^{3+} was successfully attached to TiO_2.

3.6 Photovoltaic Properties

Fig. 5 (a) shows the I-V characteristics of the dry cell for various percentage of $Al_2(SO_4)_3$ in all ADTPs in comparison to the UD-TiO_2 photoelectrode. As regards to the ADTP photoelectrode, at any point of anode voltage (V), the current (I) was always higher compared to the current of the lower doped ADTP and also UD-TiO_2. This higher current implies that the conductivity, as well as interfacial resistance of ADTP film, is better compared to the UD-TiO_2 due to $Al_2(SO_4)_3$ doping. It was corroborated by several prior investigations on doping to the TiO_2, which documented the enhancements in the conductivity of solid state DSSC when a p-type dopant was used, and determined that the dopant can impact the device's efficiency [53]. Furthermore, doping effectively suppresses the recombination loss [34] and thus with the optimum doping dosage, the conductivity of TiO_2 can be enhanced [35-37]. This conductivity improvement was beneficial for optoelectronic, photocatalytic applications and microelectronic [38][39].

Photovoltaics characterization is performed in order to investigate the influence of interface modification due to ADTP on the photovoltaic performances of complete DSSCs cells. The current density–voltage (J–V) characteristics are shown in Fig. 5 (b), and its photovoltaic properties are tabulated in Table 1. As can be witnessed, all ADTP-based DSSC exhibits an increase in the open circuit voltage (Voc), photocurrent current density (Jsc), and power conversion efficiency (PCE), as compared to UD-TiO_2-based DSSC. The Jsc, Voc, and PCE of the 1-ADTP-based DSSC are 0.84 mA/cm2, 0.58 V, 62.58 %, and 0.30 %, respectively. Notably, the 3-ADTP-based DSSC exhibited the highest PCE among other cells with Jsc, Voc, FF and PCE of 1.19 mA/cm2, 0.59 V, 67.37%, and 0.47%, respectively.

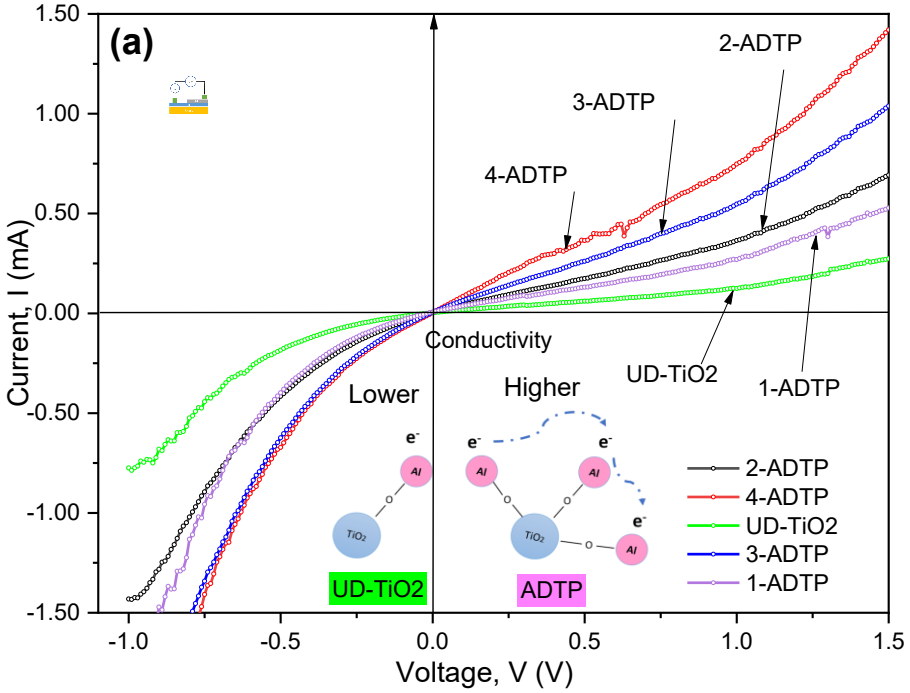

TPM Vol. 32, No. S8, 2025
ISSN: 1972-6325
https://www.tpmap.org/

Open Access

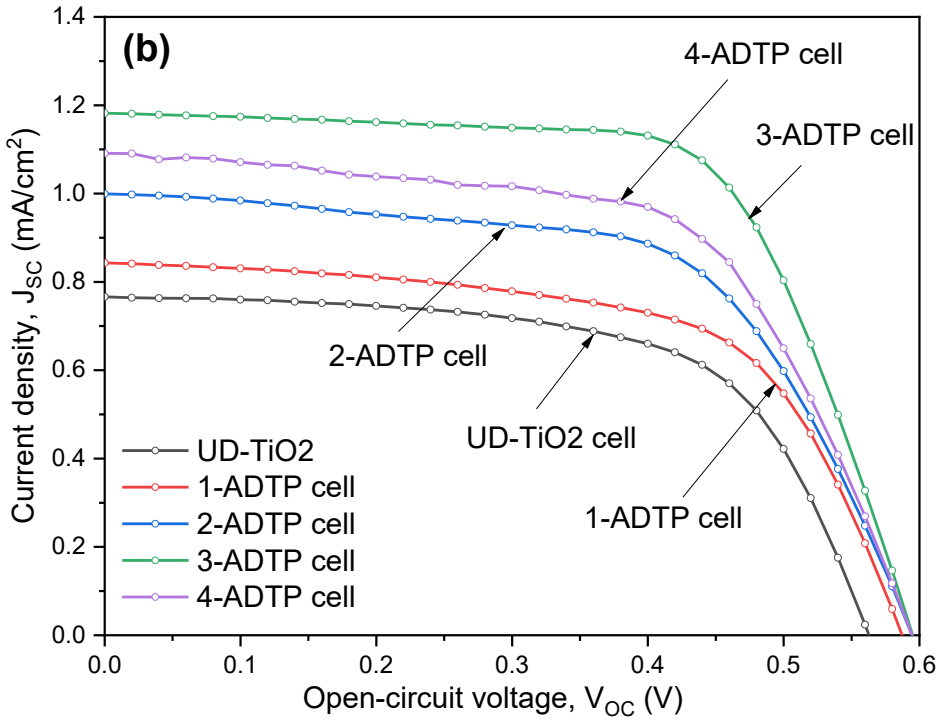

Fig. 5. Photocurrent -voltage plot, J-V curve for (a) UD-TiO_2 and ADTP photoelectrode (dry cell), (b) UD-TiO_2-based DSSC and ADTP-based DSSC (wet cell)

Table 1 Photovoltaic properties of ADTP-based DSSCs with respect to UD-TiO_2

	Jsc (mA/cm^2)	**Voc (V)**	**FF (%)**	**Efficiency (%)**
UD-TiO_2	0.76	0.56	62.93	0.27±0.02
1- ADTP-based DSSC	0.84	0.58	62.58	0.30±0.02
2- ADTP-based DSSC	1.00	0.59	61.47	0.36±0.03
3- ADTP-based DSSC	1.19	0.59	67.37	0.47±0.01
4- ADTP-based DSSC	1.10	0.59	60.83	0.39±0.02

Standard deviation calculated from three samples measured under simulated irradiation of AM 1.5 G (100 mW/cm 2).

Notably, the 3-ADTP-based DSSC exhibited the highest PCE among other cells with Jsc, Voc, FF and PCE of 1.19 mA/cm2, 0.59 V, 67.37%, and 0.47%, respectively. The higher Jsc recorded in this section is also in good agreement with the increased dye adsorption attributed to the higher $Al(OH)_3$ mediators discussed in FTIR measurement. In addition, as more$Al_2(SO_4)_3$ was added into crystal, this will introduce more carriers for electron conduction, hence further lowering the interfacial resistance. It was reported that Al-doping to the TiO_2 caused oxygen deficiencies in the crystal unit and improves interconnects between particles and hence facilitates the diffusion of atoms [40][41]. Also, the lower interfacial resistance observed in this I-V measurement was in agreement with the I-V of the above dry cell investigation. However, further adding the $Al_2(SO_4)_3$amount has been found to degrade the performances of the 4-ADTP-based DSSC with Jsc, Voc, FF, and efficiency were 1.10 mA/cm2, 0.59 V, 60.83 %, and 0.39%, respectively. The decrease in the PCE of the 4-ADTP-based DSSC might be attributed to the excess of $Al(OH)_3$ compounds that coexist on the surface of TiO_2 photoelectrode. It has been reported that the formation of excess $Al(OH)_3$ aggregates results in the reduction of the TiO_2 on top of the film and in contact with the aggregates, and to form Ti_2O_3 [42]. In addition, an abundance of dye molecules, along with the acidic carboxylic of the dye, will cause the TiO_2 nanoparticles to be dissolved, which will lead to the formation of insoluble complexes between the Ti+ ions and the anthocyanin dye molecules that have precipitated in the film pores [33]. Thus, due to incomplete dye adsorption, inactive dye molecules formed on the surfaces of the TiO_2 nanoparticle. Furthermore, an excessively high concentration of natural dye may promote polymerization and multilayer dye deposition.

TPM Vol. 32, No. S8, 2025
ISSN: 1972-6325
https://www.tpmap.org/

Open Access

3.7 Electrochemical Impedance Spectroscopy, EIS

Electrochemical impedance measurements were used to study the electron transfer in the TiO_2 electrode film by which the internal resistances and charge transport at the interfaces in DSSCs can be analyzed [43]. The Nyquist plots of UD-TiO_2 and respective ADTP-based DSSC with different doping concentrations of $Al_2(SO_4)_3$ are shown in Fig. 6 (a). The measured impedance data of DSSC was fitted by using Z-View software using an equivalent circuit model as shown in the inset of Fig. 6 (a). Generally, the impedance spectrum of DSSC (Nyquist plot) mainly consists of three semicircles corresponding to the different charge transportation processes.

The high frequency region corresponds to the charge transport at counter electrode and that at the low frequency region corresponds to the diffusion of the electroactive species in the liquid electrolyte. The intermediate frequency region is attributed to the electron transport in the photoanode film and the back reaction at the photo-anode/ electrolyte interface. The electrochemical parameters and charge transport lifetime of ADTP-based DSSC with respect to UD-TiO_2 based DSSCs is stabulated in Table 2. Generally, the EIS spectrum consists of Rs, R1, and R2, corresponding to the high frequency intercept of the first semicircle owing to the transport resistance of ITO, TiO_2/dye/electrolyte, and electrolyte/Pt electrode interface, respectively. As can be seen from the plot, the R1 and R2 value of the UD-TiO_2 was higher than all of the ADTP-based DSSC. These higher resistance components were attributed to the higher interfacial resistance of the UD-TiO_2 photoelectrode compared to the ADTP-based DSSC counterpart. Upon the introduction of $Al_2(SO_4)_3$ for the case of 1-ADTP-based DSSC to 3-ADTP-based DSSC, the interfacial resistance of the cell gets decreased, which induces rapid electron hopping (less boundary resistance) through direct bonding and Ti^{3+} trap states. This lower interfacial resistance seen in this section is strongly in agreement with the I-V measurement of the respective dry cell, as discussed in the earlier section. However, because of the increased $Al_2(SO_4)_3$ doping concentration in the 4-ADTP-based DSSC, interfacial resistance is observed to be greater than in the previous ADTP-based DSSC. This situation might be attributed to the $Al_2(SO_4)_3$ overdosing in the 4-ADTP-based DSSC have caused higher density Ti^{3+} trap states, which could permanently trap electrons [44]. The concentration of defect states in TiO_2 photoanodes has a significant impact on electron recombination in DSSC. In addition, the doping of $Al_2(SO_4)_3$provides Ti-Al (Ti-Al$(OH)_3$) direct bonding which is advantageous for the transportation of electrons over a longer distance due to reduced diffusive hindrance [13]. The interconnected TiO_2-Al also gives a greater number of electron pathways during conduction, and dye attachment sites which may favor improved charge injection and higher dye adsorption towards greater photocurrent density, Jsc. However, once overdosing, a higher doping amount will result in higher oxygen vacancy-Ti^{3+} concentrations that could lead to recombination centers of electron-hole pairs, which reduced the performance of DSSCs [45]. When compared to other DSSCs, the 3-ADTP-based DSSC has a suitable TiO_2-Al ($Al_2(SO_4)_3$ concentration) ratio, which reduces transport resistance and ultimately improves electron lifetime.

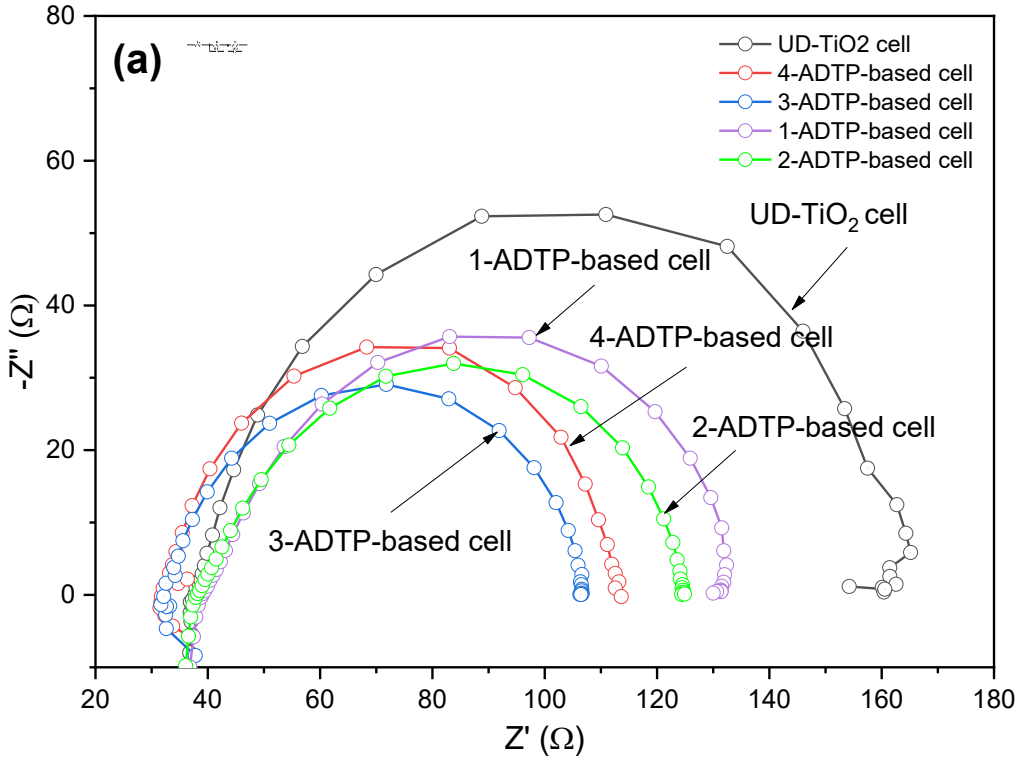

Fig. 6. (a) EIS-Nyquist plots of UD-TiO_2 and the respective ADTP-based DSSC.

Table 2 Electrochemical parameters and charge transport lifetime of ADTP-based DSSC with respect to UD-TiO_2 based DSSCs

Sample cell	Rs Ω	R1 Ω	R2 Ω	τ(ms)
UD-TiO_2	38.0	11.0	110.0	0.21
1-ADTP-based DSSC	37.5	6.1	86.0	0.25
2- ADTP-based DSSC	38.5	5.2	81.0	0.26
3- ADTP-based DSSC	38.0	3.5	71.0	2.00
4- ADTP-based DSSC	37.0	4.5	75.0	0.31

4.0 CONCLUSION

In conclusion, the tri-functional ADTP-based passivation photoelectrode was successfully investigated and proved to be a promising method of improving DSSCs. ADTP-based TiO_2 photoelectrode was created by combining TiO_2 nanoparticles and $Al_2(SO_4)_3$ salt at a specific weight percentage, and their elemental composition was confirmed using EDS analysis. The slight differences in FESEM morphological images between the two samples indicate that Ti4+ ions have been mixed and replaced by Al^{3+} ions. In the meantime, it can be seen from the photovoltaics characteristics I-V and EIS measurement that $Al_2(SO_4)_3$ doping established higher conductivity TiO_2 film. This promotes more carriers for electron conduction, which results in a further increase in photocurrent density, J_{SC}, as well as a reduction in interfacial resistance. The lower interfacial resistance is caused by rapid electron hopping, which significantly leads to a lower boundary resistance. The presence of direct bonding and Ti^{3+} trap states in the film enables these reactions. The integrated properties of the tri-functional ADTP photoelectrode, which improve interfacial resistance, induce higher dye adsorption and reduce back electrons recombination of the DSSC. Finally, it has contributed to the improvement of the 3-ADTP-based DSSC, which exhibited the highest PCE among other cells with Jsc, Voc, FF and PCE of 1.19 mA/cm2, 0.59 V, 67.37%, 0.47%, respectively.

Acknowledgement
The authors would like to thank Universiti Teknologi Mara (UiTM) Permatang Pauh, Pulau Pinang and Universiti Sains Malaysia (USM) Pulau Pinang for their research facilities. This research is financially supported by the Ministry of Higher Education of Malaysia through Fundamental Research Grant Scheme (FRGS-2019-1) (ID no 284362-301651).

REFERENCES

[1] B. Ünlü and M. Özacar, "Effect of Cu and Mn amounts doped to TiO2 on the performance of DSSCs," Sol. Energy, vol. 196 (2020) 448–456
[2] S. Mehra et al., "A review on spectral converting nanomaterials as a photoanode layer in dye-sensitized solar cells with implementation in energy storage devices," Energy Storage, vol. 2, (2) (2020) 1–28.
[3] S. G. Adhikari, A. Shamsaldeen, and G. G. Andersson, "The effect of TiCl4 treatment on the performance of dye-sensitized solar cells," J. Chem. Phys., vol. 151 (16) (2019)
[4] K. Basu et al., "Enhanced photovoltaic properties in dye sensitized solar cells by surface treatment of SnO_2 photoanodes," Sci. Rep., vol. 6, (2016) 1–10
[5] J. Tak Kim and S. Ho Kim, "Surface modification of TiO2 electrode by various over-layer coatings and O_2 plasma treatment for dye sensitized solar cells," Sol. Energy Mater. Sol. Cells, vol. 95 (1) (2011) 336–339,
[6] Y. He, J. Hu, and Y. Xie, "High-efficiency dye-sensitized solar cells of up to 8.03% by air plasma treatment of ZnO nanostructures," Chem. Commun., vol. 51 (90) (2015) 16229–16232, 2015.
[7] E. Palomares, J.N. Clifford, S.A. Haque, T. Lutz, J.R. Durrant, Control of charge recombination dynamics in dye sensitized solar cells by the use of conformally deposited metal oxide blocking layers, J. Am. Chem. Soc. 125 (2003) 475–482.
[8] J.R. Durrant, S.A. Haque, E. Palomares, towards optimisation of electron transfer processes in dye sensitised solar cells, Coordin. Chem. Rev. 248 (2004) 1247–1257.
[9] H.J. Snaith, C. Ducati, SnO2-based dye-sensitized hybrid solar cells exhibiting near unity absorbed photon-to-electron conversion efficiency, Nano Lett. 10 (2010) 1259–1265.
[10] F. Huang, Y.-B. Cheng, R.A. Caruso, Al-doped TiO2 Photoanode for Dye-Sensitized Solar Cells, Aust. J. Chem. 64 (2011) 820–824.
[11] E. Palomares, J.N. Clifford, S.A. Haque, T. Lutz, J.R. Durrant, Control of charge recombination dynamics in dye sensitized solar cells by the use of conformally deposited metal oxide blocking layers, J. Am. Chem. Soc. 125 (2002) 475–482.
[12] S.G. Chen, S. Chappel, Y. Diamant, A. Zaban, Preparation of Nb2O5 coated TiO2 nanoporous electrodes and their application in dye-sensitized solar cells, Chem. Mater. 13 (2001) 4629–4634.

[13] T. Kirthi, B. Jayasundara, B. Priyangi Konara Mudiyanselage, K. Gamaralalage Rajanya Asoka, K. Akinori, Enhanced efficiency of a dye-sensitized solar cell made from MgO-coated nanocrystalline SnO2, Jpn. J. Appl. Phys. 40 (2001) L732.
[14] Hyun Suk Jung, Jung-Kun Lee, Sangwook Lee, Kug Sun Hong, Hyunho Shin, Acid adsorption on TiO2 nanoparticles – an electrochemical properties study, J. Phys. Chem. C 112 (22) (2008) 8476–8480.
[15] Park, Kyung-Hee, et al. "Effects of HNO3 treatment of TiO2 nanoparticles on the photovoltaic properties of dye-sensitized solar cells." Materials Letters 63.26 (2009): 2208-2211.
[16] Zhong-Sheng Wang, Takeshi Yamaguchi, Hideki Sugihara, Hironori Arakawa, Significant efficiency improvement of the black dye-sensitized solar cell through protonation of TiO2 films, Langmuir 21 (10) (2005) 4272–4276.
[17] B.C. O'Regan, J.R. Durrant, P.M. Sommeling, N.J. Bakker, Influence of the TiCl4 treatment on nanocrystalline TiO2 films in dye-sensitized solar cells. 2. Charge density, band edge shifts, and quantification of recombination losses at short circuit, J. Phys. Chem. C 111 (2007) 14001–14010
[18] V. L. Punzi, V. Z. Kungne, and D. W. Skaf, “Removal of titanium dioxide nanoparticles from wastewater using traditional chemical coagulants and chitosan,” Environ. Prog. Sustain. Energy, no. June 2019, 2020.
[19] R. Kashyap, N. Sharma, and L. Sharma Divya, “Dyeing of Cotton with Natural Dye Extract from Coconut Husk,” IJSTE-International J. Sci. Technol. Eng. |, vol. 3, no. 04, pp. 92–95, 2016.
[20] M. Bouloudenine, et al., Zn1− xCoxO diluted magnetic semiconductors synthesized under hydrothermal conditions, Catal. Today 113 (3–4) (2006) 240–244. [29] J. Singh, et al., Synthesis, band-gap tuning, structural and optical investigations of Mg doped ZnO nanowires, Cryst.Eng. Comm 14 (18) (2012) 5898–5904.
[21] J. Singh, et al., Synthesis, band-gap tuning, structural and optical investigations of Mg doped ZnO nanowires, Cryst. Eng. Comm 14 (18) (2012) 5898–5904.
[22] F. Davar, M.R.L. Estarki, M.S. Niasari, R. Ashiri, Int. J. Appl. Ceram. Technol. 11 (4) (2014) 637–644.
[23] Abdullah, M. H., et al. "Synergistic effect of complementary organic dye co-sensitizers for potential panchromatic light-harvesting of dye-sensitized solar cells." Optical Materials 133 (2022): 113016.
[24] C.-C. Yen, et al., A combined experimental and theoretical analysis of Fe-implanted TiO2 modified by metal plasma ion implantation, Appl. Surf. Sci. 256 (22) (2010) 6865–6870.
[25] M. Alias, K.M. Rashid, K. Adem, Optical properties for Ti doped thin Zno films prepared by PLD, Int. J. Innovat. Res. Sci. Eng. Technol. 3 (8) (2014) 15538–15544.
[26] R.J. Alvaro, ´ N.D. Diana, A.M. María, Effect of Cu on optical properties of TiO2 nanoparticles, Contemp. Eng. Sci. 10 (2017) 1539–1549. by direct precipitation method, Superlattice. Microst. 85 (2015) 7–23.
[27] Subki, A. S. R. A., Mamat, M. H., Mohamed Zahidi, M., Abdullah, M. H., Shameem Banu, I. B., Vasimalai, N., ... & Mahmood, M. R. (2022). Optimization of aluminum dopant amalgamation immersion time on structural, electrical, and humidity-sensing attributes of pristine ZnO for flexible humidity sensor application. Chemosensors, 10(11), 489.
[28] Khan, A. A., et al. "Magnesium sulfate as a potential dye additive for chlorophyll-based organic sensitiser of the dye-sensitised solar cell (DSSC)." Spectrochimica Acta Part A: Molecular and Biomolecular Spectroscopy 274 (2022): 121140.
[29] Shahrul, A. M., et al. "Low-cost coagulation treatment of dye sensitizer for improved time immersion of dye-sensitized solar cells (DSSC)." Microelectronic Engineering 262 (2022): 111832.
[30] Shahrul, A. M., et al. "Synergistic role of aluminium sulphate flocculation agent as bi-functional dye additive for Dye-Sensitized Solar Cell (DSSC)." Optik 258 (2022): 168945.
[31] E.M. Jin, K.-H. Park, B. Jin, J.-J. Yun, H.-B. Gu, Photosensitization of nanoporous TiO2 films with natural dye, Phys. Scr. T139 (2010) 14006
[32] M.K. Nazeeruddin, R. Humphry-Baker, D.L. Officer, W.M. Campbell, A.K. Burrell, M. Gratzel, Application of metalloporphyrins in nanocrystalline 306 G.D. Sharma et al. / Organic Electronics 25 (2015) 295–307 dye-sensitized solar cells for conversion of sunlight into electricity, Langmuir 20 (2004) 6514–6517
[33] Shahrul, A. M., et al. "Coactive impact of a novel multifunctional alum co-adsorbent for dye-sensitized solar cells DSSC." Materials Letters 317 (2022): 132088.
[34] M. Asemi and M. Ghanaatshoar, “Influence of TiO2 particle size and conductivity of the CuCrO 2 nanoparticles on the performance of solid-state dye-sensitized solar cells,” vol. 40, no. 7, pp. 1379–1388, 2017.
[35] Arof, S., Noorsal, E., Yahaya, S. Z., Hussain, Z., Mohd Ali, Y., Abdullah, M. H., & Safie, M. K. (2023). Adaptive sliding mode feedback control algorithm for a nonlinear knee extension model. Machines, 11(7), 732.
[36] Lyly Nyl, Ismail, et al. "Optical properties and surface morphology of PMMA: TiO2 nanocomposite thin films." Advanced Materials Research 364 (2012): 105-109..
[37] Rahman, M. Atowar. "Enhancing the photovoltaic performance of Cd-free Cu2ZnSnS4 heterojunction solar cells using SnS HTL and TiO2 ETL." Solar Energy 215 (2021): 64-76.

[38] S. B. Nair, K. Aijo John, H. Rahman, J. A. Joseph, S. K. Remillard, and R. R. Philip, “Aluminium doping-a cost effective and super-fast method for low temperature crystallization of TiO 2 nanotubes,” CrystEngComm, vol. 21, (1), (2019) 128–134
[39] V. Krishnakumar, S. Boobas, J. Jayaprakash, M. Rajaboopathi, B. Han, and M. Louhi-Kultanen, “Effect of Cu doping on TiO2 nanoparticles and its photocatalytic activity under visible light,” J. Mater. Sci. Mater. Electron., vol. 27 (7) 2016) 7438–7447,
[40] Choi, Young Jin, et al. "Aluminum-doped TiO2 nano-powders for gas sensors." Sensors and Actuators B: Chemical vol. 124 (1) (2007): 111-117.
[41] K. Hatta, M. Higuchi, J. Takahashi, K. Kodaira, J. Cryst. Growth 1996, 163, 279.
[42] Y.-J. Liou, Y.J. Chen, B.-R. Chen, L.-M. Lee, C.-H. Huang, XPS study of aluminum coating on TiO2 anode of dye-sensitized solar cells, Surf. Coat. Technol. 231 (2013) 535–538.
[43] Ismail, L. N., Mohamad, N. N. H. N., Shamsudin, M. S., Zulkefle, H., Abdullah, M. H., Herman, S. H., & Rusop, M. (2012). Effect of solvent on the dielectric properties of nanocomposite poly (methyl methacrylate)-doped titanium dioxide dielectric films. Japanese Journal of Applied Physics, 51(6S), 06FG09.
[44] Roose, B., Pathak, S., Steiner, U., 2015. Doping of TiO2 for sensitized solar cells. Chem. Soc. Rev. 44, 8326–8349.
[45] J. Weidmann, T. Dittrich, E. Konstantinova, I. Lauermann, I. Uhlendorf, F. Koch, Influence of oxygen and water related surface defects on the dye sensitized TiO2 solar cell, Sol. Energy Mat. Sol. Cells 56 (1999) 153–165.
[46] McCafferty, E. W. J. P., and J. P. Wightman. "Determination of the concentration of surface hydroxyl groups on metal oxide films by a quantitative XPS method." Surface and Interface Analysis: An International Journal devoted to the development and application of techniques for the analysis of surfaces, interfaces and thin films 26.8 (1998): 549-564.